Membrane Modulates Affinity for Calcium Ion to Create an Apparent Cooperative Binding Response by Annexin a5

Jacob W. Gauer,[†△] Kristofer J. Knutson,[†△] Samantha R. Jaworski,[†] Anne M. Rice,[†] Anika M. Rannikko,[†] Barry R. Lentz,[‡] and Anne Hinderliter[†*]

[†]Department of Chemistry and Biochemistry, University of Minnesota Duluth, Duluth, Minnesota; and [‡]Department of Biochemistry and Biophysics, University of North Carolina, Chapel Hill, North Carolina

ABSTRACT Isothermal titration calorimetry was used to characterize the binding of calcium ion (Ca^{2+}) and phospholipid to the peripheral membrane-binding protein annexin a5. The phospholipid was a binary mixture of a neutral and an acidic phospholipid, specifically phosphatidylcholine and phosphatidylserine in the form of large unilamellar vesicles. To stringently define the mode of binding, a global fit of data collected in the presence and absence of membrane concentrations exceeding protein saturation was performed. A partition function defined the contribution of all heat-evolving or heat-absorbing binding states. We find that annexin a5 binds Ca^{2+} in solution according to a simple independent-site model (solution-state affinity). In the presence of phosphatidylserine-containing liposomes, binding of Ca^{2+} differentiates into two classes of sites, both of which have higher affinity compared with the solution-state affinity. As in the solution-state scenario, the sites within each class were described with an independent-site model. Transitioning from a solution state with lower Ca^{2+} affinity to a membrane-associated, higher Ca^{2+} affinity state, results in cooperative binding. We discuss how weak membrane association of annexin a5 prior to Ca^{2+} influx is the basis for the cooperative response of annexin a5 toward Ca^{2+}, and the role of membrane organization in this response.

INTRODUCTION

At its simplest, the membrane is a barrier. This barrier fundamentally enables the compartmentalization of distinct chemical processes, a trait that is one of the primary differences between eukaryotes and prokaryotes. At its most complex, we suggest that the components of the membrane, based upon their organization, have the capacity to transduce cellular signaling by altering protein-protein, protein-lipid, and lipid-lipid interactions (1,2). The primary components of the biomembrane, lipids and proteins, distribute nonideally to optimize favorable contacts and minimize free energy. Thus, the structural organization of the membrane impacts the information flow of signaling into and out of the eukaryotic cell. The ability of membranes to provide a responsive surface by virtue of the weak yet cooperative interactions between lipids allows signals to be amplified at the membrane surface by readily altering the distribution of membrane-associated proteins (3). In this way, lipid membranes are not simply a surface upon which proteins adhere—they are also able to sensitively modulate the affinity of protein for this surface via changes in how the lipids interact with one another within the membrane. This is due to the thermodynamic activity (or effective concentration) of lipids, which is dependent on the composition of the lipid mixture (4).

Here we propose that these disparate functions of the cellular membrane (barrier, surface, and signal tuning) unite to position a peripheral-membrane-binding protein to respond to calcium ion (Ca^{2+}) influx in a cooperative manner. Furthermore, we propose that the family of proteins called the annexins utilize this cooperative response to modulate access of other proteins to the membrane surface and thereby regulate the membrane's ability to transduce cellular signaling information. Through the use of linkage relationships and a global approach to fitting a thermodynamic cycle, we ascertained the impact of membrane association on Ca^{2+} binding, and the impact of Ca^{2+} binding on membrane association, for annexin a5. We find that it is the weak interaction of annexin a5 with the membrane surface before a Ca^{2+} influx that enables the apparent cooperative binding of Ca^{2+}.

The annexins, of which there are 11 forms in humans, share a core domain consisting of repeating α-helices (5). Annexins are known to have a variety of binding partners, including acidic-phospholipid-containing membranes and Ca^{2+} (6). Extensive work has characterized these binding interactions; however, a consistent model is lacking (7–22). Although they account for some 2% of all intracellular protein, the exact functions of annexins are unknown. This notable abundance suggests a defined cellular role that merits such high expression levels. The annexins are an ancient family of proteins that are highly conserved throughout evolutionary history, implying a primary function in the cell. One study identified an ancestral protein, possibly an annexin predecessor, as part of a model of annexin evolution, and found that membrane association rather than Ca^{2+} binding was the crucial property necessary for function (23). We suggest that the annexins have not only conserved their ability to interact with membranes but have also tuned this ability such that they can modulate

Submitted February 19, 2013, and accepted for publication March 20, 2013.

△Jacob W. Gauer and Kristofer J. Knutson contributed equally to this work.

*Correspondence: ahinderl@d.umn.edu

Editor: Heiko Heerklotz.

0006-3495/13/06/2437/11 $2.00

http://dx.doi.org/10.1016/j.bpj.2013.03.060

membrane organization through weak lipid-lipid, lipid-protein, and protein-protein interactions (24–27).

In earlier work (28), we revealed the linkage between cation and membrane binding to annexin a5 by using a Ca^{2+} mimic, terbium (Tb^{3+}), and taking advantage of the quenching of endogenous fluorescence of annexin a5 upon Tb^{3+} binding. We found that an allosteric transition model fit the experimental data showing that protein bound to membranes containing acidic phospholipid had increased affinity for cation compared with protein in solution. We proposed that a shift to higher cation affinity when the protein was membrane associated conveyed the apparent cooperativity. This proposed model was not in agreement with existing binding models for the annexins, as a wide variety of experimental approaches have instead led to the conclusion that annexins are Ca^{2+}-dependent, membrane-binding proteins (17,21,29–30).

We hypothesized that annexins regulate membrane accessibility (lipid distribution) and hence the assembly of signaling complexes at the membrane surface (24). However, the associated affinities reported in the literature varied widely, ranging from extremely high to very low (8,15,29). The reported distribution of binding affinities with Ca^{2+} and phospholipid implies a distribution of membrane occupancies that then becomes model dependent. To test this hypothesis, we must have a predictive ability to calculate membrane occupancy under a variety of lipid compositions in response to Ca^{2+} influx. Membrane-based signaling is often triggered by Ca^{2+} influx (2), and the membrane-enhanced response of the annexins to Ca^{2+} suggests coupling between membrane organization and Ca^{2+} influx. Thus, it was necessary to resolve the complex, linked binding of Ca^{2+} and membrane by annexin. In existing binding models, it is proposed that the presence of Ca^{2+} induces membrane binding, primarily based on the observation that annexins have a greater affinity for Ca^{2+} in the presence of membrane than in the absence of membrane. We had noted a similar binding behavior with Tb^{3+}; however, within the context of a thermodynamic cycle, a more complex picture emerged. A weak association with the membrane was the basis of this cooperative cation-binding response (28). It was unknown whether this result might be attributed to the use of a Ca^{2+} mimic, Tb^{3+}. We reexamined the binding of annexin a5 using isothermal titration calorimetry (ITC), a method that allows the binding behavior of annexin's endogenous ligands of Ca^{2+} and membrane to be precisely defined from a partition function formalism (31). We selected the simplest annexin with which to begin: annexin a5. This annexin has a highly conserved binding core and the shortest variable N-termini, which eliminates additional complexity in its binding behavior (6,32–34). We previously found similarities in binding behavior between annexin a5 and a4, suggesting that binding similarities were retained within their conserved core (28).

The heat of each experimental Ca^{2+} titration point with ITC is the direct manifestation of a redistribution of the bound and unbound states of annexin under increasing saturation of Ca^{2+} in the presence and absence of phospholipid. Conversely, the heat of each experimental membrane titration point is due to the redistribution of the bound and unbound states of annexin upon increasing saturation with membrane surface while in the presence and absence of Ca^{2+}. To define the binding models, we varied the protein concentrations, ligand concentrations, membrane composition, and membrane concentrations for titration replicates. In a given titration, the enthalpy, the number of binding sites, and the association constant are fit parameters. By utilizing the thermodynamic cycle of binding, we constructed a partition function that represented all possible states in which the protein could exist (bound or unbound). Partition functions allow binding models to be derived, and each proposed binding model was tested against the combined data sets. Binding models were derived in increasing complexity with the minimum number of binding constants that described all sides of the thermodynamic cycle (Fig. 1). The combined calculated free energies and fitted values of enthalpy were also checked against the thermodynamic cycle. The sum of all free energies in a cycle was zero. One model, the allosteric transition model, was found to meet all of these screening criteria. Essentially, this model is a variant of the original Monod-Wyman-Changuex (MWC) model of allosterism (Fig. 2). Although such models are being applied to some classes of integral membrane receptors to qualitatively describe their biological response (50–54), we are unaware of such a model being proposed for peripheral-membrane proteins.

The basis of this proposed allosteric transition model is that the small population of protein that is membrane associated in the absence of Ca^{2+} enables the cooperative Ca^{2+}-binding response. As in the MWC model, there are two states: in one state, annexin is membrane associated, and in the other it is free in solution. Although the membrane-associated state has greater affinity for Ca^{2+} before the introduction of Ca^{2+}, its relative concentration is very low

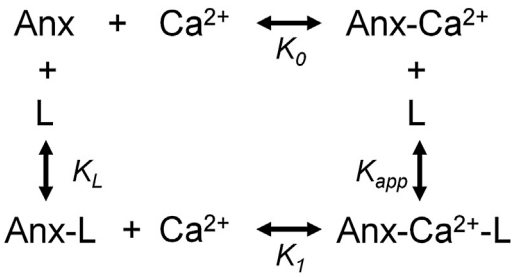

FIGURE 1 Annexin a5 thermodynamic cycle. Annexin Ca^{2+} binding differentiates into two classes of Ca^{2+} sites in the presence of membrane: K1a and K1b (for simplification, this is illustrated as K1; for a more detailed representation of all of the states, see Fig. 2).

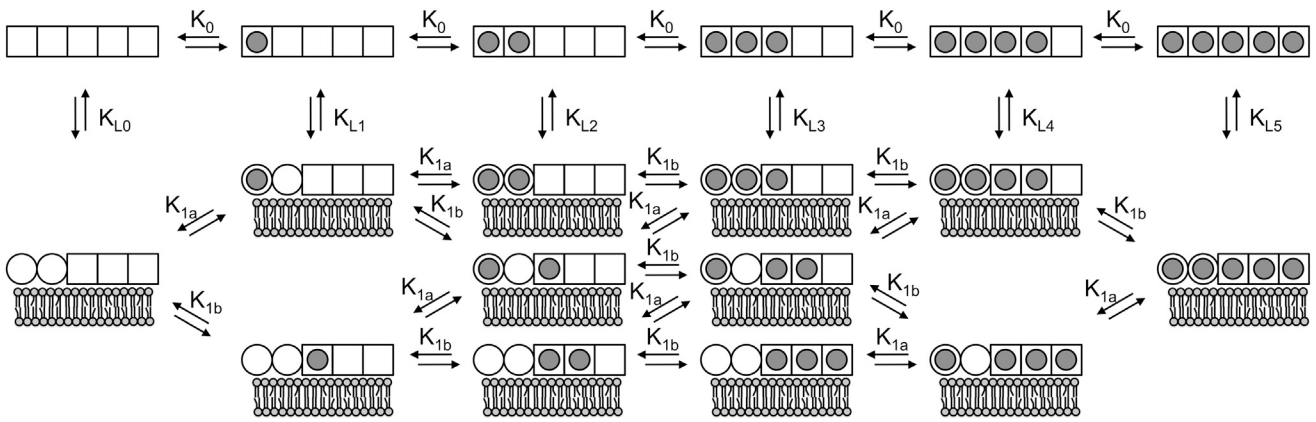

FIGURE 2 Schematic of all potential species involved in the model for binding of Ca^{2+} and membrane to annexin. The model is analogous to the MWC model of O_2 binding hemoglobin (48), where the MWC states tensed (T) and relaxed (R) are replaced by solution and membrane-bound states. In the absence of membrane, all five Ca^{2+} sites are low affinity (K_0) and exothermic (represented as *squares*). In the presence of membrane, the five Ca^{2+}-binding sites differentiate into two classes: two high-affinity (K_{1a}) endothermic Ca^{2+} sites (represented as *circles*) and three low-affinity (K_{1b}) exothermic Ca^{2+} sites (represented as *squares*). Transitioning to the membrane-bound state in the absence of Ca^{2+} is dictated by the affinity K_L, which is analogous to the equilibrium constant describing the transition between the T and R states in the MWC model. As in the classic MWC model, in each state (solution or membrane-bound), binding sites are considered to be independent and equivalent within each class.

compared with solution-state (nonmembrane-associated) annexin. Instead of multiple subunits, each with a single binding site, as in the MWC model, here there are multiple binding sites for ligand in each state of the protein. A critical component of this model, the weakly membrane-associated state of annexin a5 in the absence of Ca^{2+} and enhanced membrane association in the presence of Ca^{2+}, has been directly observed with the use of fluorescence microscopy and ITC (25,35). Our analysis reveals that this membrane-associated population of protein binds Ca^{2+} with greater affinity compared with solution affinity, and that membrane association differentiates the calcium sites into two classes. This model is also consistent with annexins appearing as Ca^{2+}-dependent, membrane-binding proteins due to the observed cooperative Ca^{2+}-binding response. Before a Ca^{2+} influx occurs, the annexin is primarily in solution and binding of Ca^{2+} increases the affinity of the protein for membrane. Thus, the probability of a membrane- and Ca^{2+}-bound state of the protein increases. Upon binding to membrane, the low-affinity Ca^{2+} sites become high-affinity sites, which also increases the binding probability of additional low-affinity Ca^{2+} sites. We propose that this transition from low affinity (solution) to high affinity (membrane) is the basis of the observed cooperative binding of annexin to Ca^{2+} in the presence of membrane. Previous observations that other calcium-binding proteins have a weak membrane association in the absence of Ca^{2+} (36–37) suggest that this proposed model may extend beyond the annexins.

MATERIALS AND METHODS

All materials and methods used in this work are described in the Supporting Material.

MODEL

The molecular semigrand canonical partition function that represents the distribution of molecular states relative to the ligand-free state is calculated as

$$Q = \left(1 + K_0\left[Ca^{2+}\right]\right)^5 + K_L[L]\left(1 + K_{1a}\left[Ca^{2+}\right]\right)^2 \times \left(1 + K_{1b}\left[Ca^{2+}\right]\right)^3 \quad (1)$$

The solution-state population of Ca^{2+} is represented by $(1 + K_0[Ca^{2+}])^5$, where K_0 is the affinity of equal and independent Ca^{2+}-binding sites on annexin. The population of membrane-bound annexin for Ca^{2+} is $K_L[L]\ (1 + K_{1a}[Ca^{2+}])^2\ (1 + K_{1b}[Ca^{2+}])^3$, where $(1 + K_{1a}[Ca^{2+}])^2$ reflects a high-affinity class of two equivalent and independent Ca^{2+}-binding sites of affinity K_{1a}, and $(1 + K_{1b}[Ca^{2+}])^3$ similarly reflects a lower-affinity class of three equivalent and independent Ca^{2+}-binding sites of affinity K_{1b}. The term $K_L[L]$ is the probability of being in the membrane-associated conformational state, as $K_L[L] = [PL]/[P]_{free}$. The fractional saturation of annexin with Ca^{2+} is then represented by all the terms associated with Ca^{2+}-ligated sites normalized by all of the possible states (the partition function). The finding of five Ca^{2+}-binding sites is within the range of cation-ligated states identified for annexin a5 (28). We determined for annexin a5 in the presence of membrane that the calcium affinities differentiate. In the presence of membranes composed of 1-palmitoyl-2-oleoyl-*sn*-glycero-3-phosphocholine (POPC)/1-palmitoyl-2-oleoyl-*sn*-glycero-3-phosphoserine (POPS) (60:40), we found that annexin a5 displays five cation sites (three low affinity and two high affinity). In the absence of membranes, only five low-affinity sites were found. Furthermore, the number of Ca^{2+}-binding

sites varied with membrane composition (see "Extension of the binding model to a physiological lipid composition" below). Annexin a1, likewise, has numerous (six) cation sites that are differentiated into high and low affinities, albeit in the absence of membrane (10).

When annexin is titrated with membrane at a fixed Ca^{2+} concentration, the resultant apparent binding constant becomes a function of Ca^{2+} concentration (K_{app} is calculated for each fixed Ca^{2+} concentration). K_{app} represents the switching of the protein from a Ca^{2+}-bound state in solution to a Ca^{2+}- and membrane-bound state. K_{app} is expressed in terms of the different equilibrium constants that describe Ca^{2+} binding (K_0, K_{1a}, and K_{1b}), the equilibrium constant that describes lipid binding in the absence of Ca^{2+} (K_L), and free Ca^{2+} concentration as

$$K_{app} = \frac{K_L(1 + K_{1a}[Ca^{2+}])^2(1 + K_{1b}[Ca^{2+}])^3}{(1 + K_0[Ca^{2+}])^5} \quad (2)$$

It is the evaluation of K_{app} from experimental data that enable the calculation of K_L. The interdependence of K_{app} and K_L is illustrated in the Supporting Material.

From the partition function (Eq. 1), the affinity of annexin in its Ca^{2+}-bound state for membrane [L] may be determined from $\Theta = [L]/Q^*dQ/d[L]$ (38). Because each liposome is a single binding site per annexin, an independent site model fits the resultant binding isotherm of

$$\Theta = \frac{K_{app}[L]}{1 + K_{app}[L]} \quad (3)$$

The fitted value of K_{app} from experimental titrations carried out at saturating or nearly saturating Ca^{2+} concentrations (see Fig. 5) allows calculation of K_L, as K_0 was previously determined from Fig. 3, and K_{1a} and K_{1b} were determined from Fig. 4. Thus, K_L could be calculated.

RESULTS

The raw data measured during the ITC experiments are shown in Figs. 3–5 (*top panel*), where each peak represents the heat of binding resulting after an injection. The integrated peak areas are plotted as a function of the ratio between the total ligand concentration and the total protein concentration (Figs. 3–5, *middle panel*). This presentation of data is standard for ITC experiments (39). Traditionally, binding isotherms are plotted in a cumulative manner as a function of free ligand [X]. Thus, the cumulative heats resulting from each injection point were normalized to the total heat of the bound state and plotted as a function of the increasing free ligand concentration (fractal saturation). Because the resultant heat of each peak is a direct manifestation of production of the bound state of annexin, by summing all these heats and normalizing the total heat of the titration after each injection to the total summed heat of the titration after saturation, we can determine the fractional saturation and then plot it as a function of free ligand (Figs. 3–5, *bottom panel*). Free ligand is calculated by subtracting the total ligand from the bound ligand as defined by the equilibrium constant (K) and the number of binding sites (n).

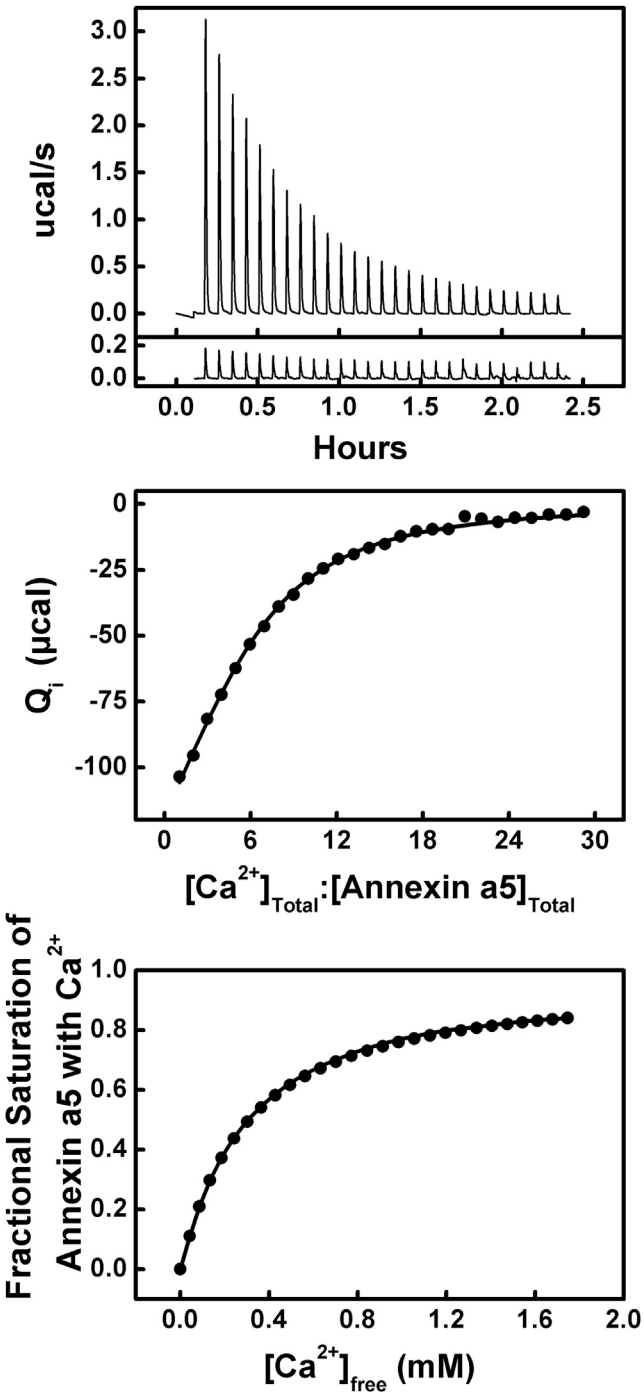

FIGURE 3 Results of the titration of 90 μM annexin a5 with Ca^{2+} at 15°C. Top: (Above) Raw ITC data. (Below) Heat of dilution data (control). Middle: Integrated heats of binding as a function of ligand/protein ratio. Bottom: Binding isotherm of fractional saturation as a function of free $[Ca^{2+}]$.

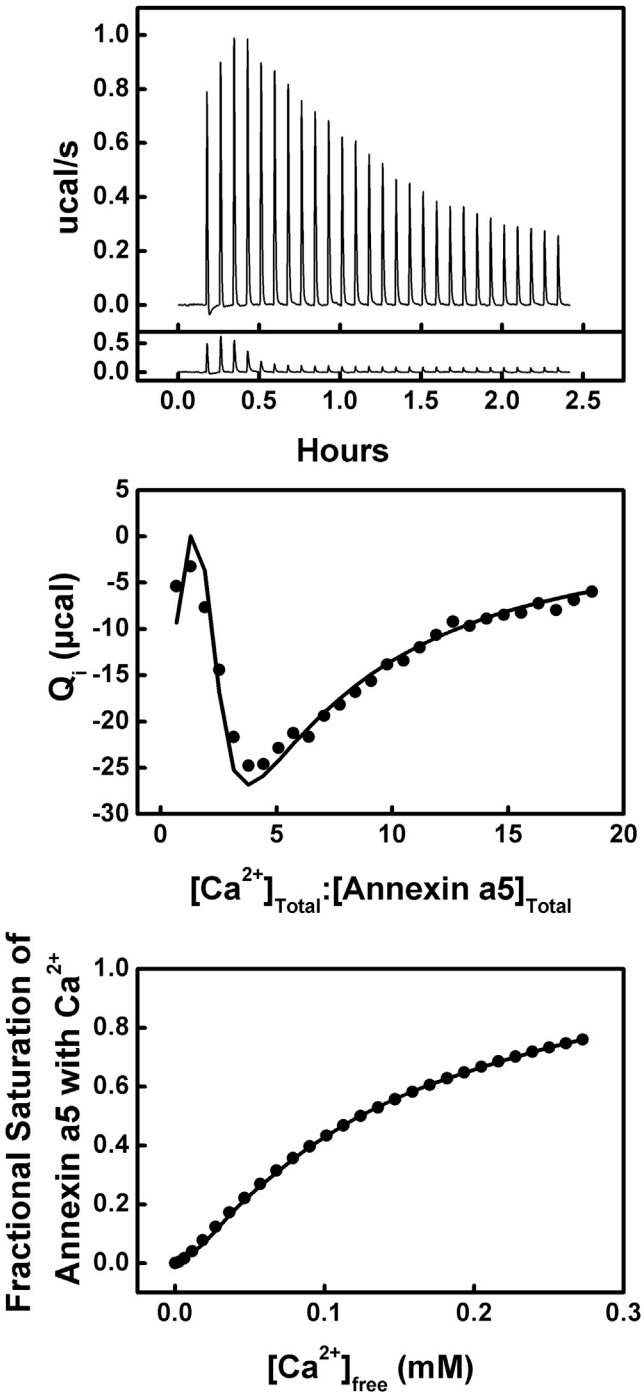

FIGURE 4 Results of the titration of 24 μM annexin a5 with Ca^{2+} in the presence of 2 mM total lipid as LUVs made of a 60:40 mixture of POPC/POPS at 18°C. Top: (Above) Raw ITC data. (Below) Heat of dilution data (control). Middle: Integrated heats of binding as a function of ligand/protein ratio. Bottom: Binding isotherm of fractional saturation as a function of free [Ca^{2+}].

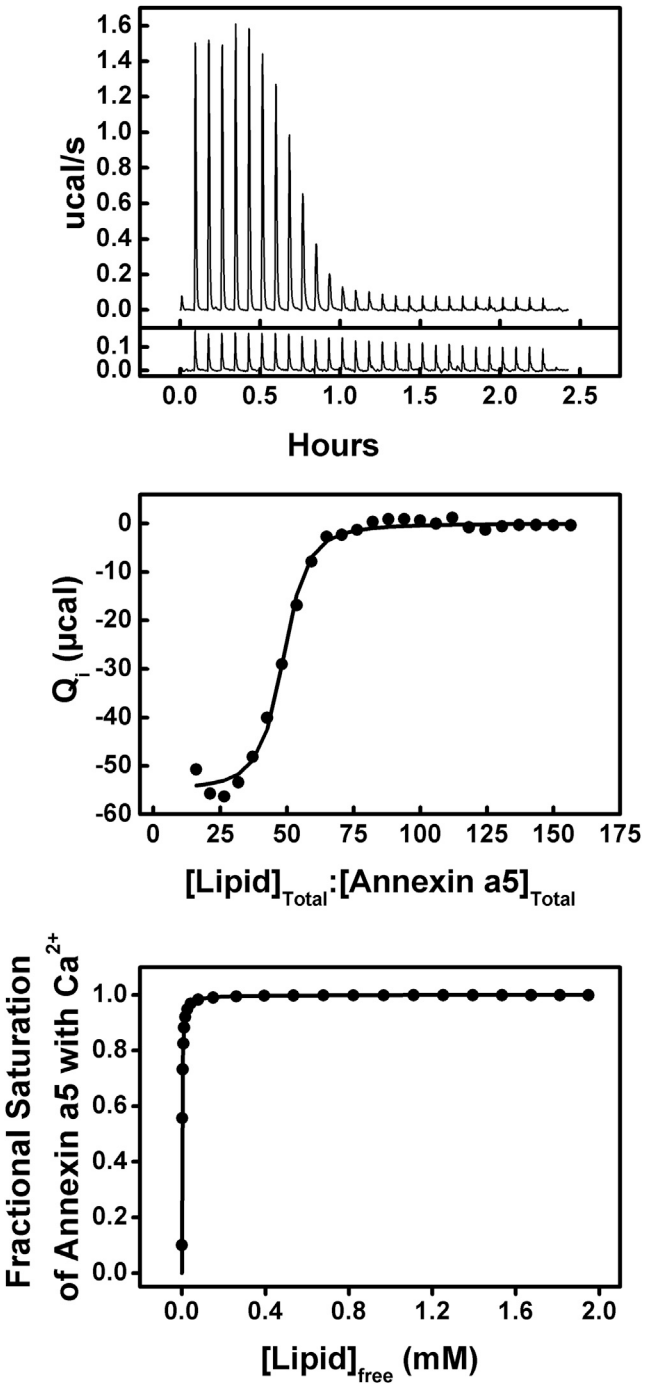

FIGURE 5 Results of the titration of 30 μM annexin a5 with lipid as LUVs made of a 60:40 mixture of POPC/POPS in the presence of 0.75 mM Ca^{2+} at 15°C. Top: (Above) Raw ITC data. (Below) Heat of dilution data (control). Middle: Integrated heats of binding as a function of ligand/protein ratio. Bottom: Binding isotherm of fractional saturation as a function of free [Lipid].

Ca^{2+} binding by annexin a5 in the absence of membrane

The titration of annexin a5 with Ca^{2+} in the absence of membrane is shown in Fig. 3. Here, the measured heat of binding was best fit using a simple binding model (see Supporting Material for details) that assumes n_0 independent Ca^{2+}-binding sites with equal affinity, K_0, and equal heat of binding, ΔH_0 (39). These three parameters were found

by nonlinear least-squares regression to be $n_0 = 5.0 \pm 0.4$, $K_0 = (3.1 \pm 0.3) \times 10^3\ M^{-1}$ ($K_{D,0} = 330 \pm 40\ \mu M$), and $\Delta H_0 = -2.4 \pm 0.2$ kcal/mole (Table 1).

Ca^{2+} binding by annexin a5 in the presence of membrane

The titration of annexin a5 with calcium in the presence of POPC/POPS (60:40) large unilamellar vesicles (LUVs) is shown in Fig. 4. The increased complexity in these data is recognizable. The two apparent trends suggest that at least two heat-exchanging processes occur with heats of opposite sign. This trend was previously reported in the C2 domains of protein kinase C with a binding isotherm similar to that shown in Fig. 4 (35). The measured heat of binding was best fit using a binding model that assumed two sets of linked Ca^{2+}-binding sites (see Supporting Material for details). In short, we assumed that of the two sets of Ca^{2+}-binding sites responsible for these observations, one consisted of n_{1a} high-affinity K_{1a} sites with endothermic heat ΔH_{1a}, and the other consisted of n_{1b} low-affinity K_{1b} sites and exothermic heat ΔH_{1b}. Furthermore, the total number of Ca^{2+} sites when membrane associated ($n_{1a} + n_{1b}$) was assumed to be conserved ($n_{1a} + n_{1b} = n_0$) compared with the number of solution Ca^{2+} sites (n_0). Deconvolution of the data was achieved by fitting the individual contributions of each set in an iterative fashion. These results suggest that there were $n_{1a} = 2.0 \pm 0.1$ sites with affinity $K_{1a} = (4.1 \pm 1.2) \times 10^5\ M^{-1}$ ($K_{D,1a} = 2.4 \pm 1.0\ \mu M$) and heat of binding $\Delta H_{1a} = 3.8 \pm 0.2$ kcal/mole (the endothermic, high-affinity sites), and $n_{1b} = 3.0 \pm 0.1$ sites with affinity $K_{1b} = (5.8 \pm 0.1) \times 10^3\ M^{-1}$ ($K_{D,1b} = 170 \pm 10\ \mu M$) and heat of binding $\Delta H_{1b} = -13.4 \pm 0.4$ kcal/mole (the exothermic, low-affinity sites; Table 1).

Membrane binding by annexin a5 in the presence of saturating Ca^{2+} and calculation of membrane binding in the absence of Ca^{2+}

The titration of annexin a5 with phospholipid membranes (LUVs composed of a 60:40 mixture of POPC/POPS) in the presence of Ca^{2+} is shown in Fig. 5. Note that at the high Ca^{2+} concentrations of this titration, only two states would dominate (annexin a5 in solution saturated with Ca^{2+} or membrane-associated annexin a5 saturated with Ca^{2+}). We used a model that described membrane binding as having affinity K_{app} and heat of membrane binding ΔH_{app}. Because we handle the stoichiometry of binding differently when considering binding to a membrane surface versus binding to small ligands, we incorporated a parameter z, which is the average binding stoichiometry of lipids per protein, instead of the parameter n that we used previously (see Supporting Material for details). Annexin binds membrane composed of a 60:40 ratio of neutral to negatively charged lipids in an LUV suspension with an affinity of $K_{app} = (7.8 \pm 0.4) \times 10^4\ M^{-1}$ ($K_{D,app} = 13 \pm 1.0\ \mu M$), a heat of binding of $\Delta H_{app} = -17.3 \pm 0.1$ kcal/mole, and an average binding stoichiometry of $z = 46.5 \pm 0.1$ lipids per protein molecule (Table 1). If a lipid has a first ring of six nearest-neighboring lipids, and then 12 nearest neighbors, 18, 24, etc., then 40–50 lipids/protein corresponds to only three to four layers of hexagonally packed lipids, which is consistent with the known size of annexin a5 (40). We carried out carboxyfluorescein efflux studies to ensure that annexin binding of the LUVs did not disrupt the membrane. In fact, binding instead appears to decrease the permeability of the membrane (see Supporting Material).

Using Eq. 2, annexin a5's membrane affinity in the absence of Ca^{2+} was calculated to be $K_L = (2.1 \pm 0.3) \times 10^1\ M^{-1}$ ($K_{D,L} = 50 \pm 20$ mM). Notice that for a given Ca^{2+} concentration, the ratio $(1 + K_{1a}[Ca^{2+}])^2\ (1 + K_{1b}[Ca^{2+}])^3 / (1 + K_0[Ca^{2+}])^5$ would be constant. Because K_{app} is directly proportional to K_L, an accurate determination of K_L is dependent on an accurate determination of K_{app}. The fit parameter K_{app} is extremely sensitive to the curvature observed in the data, as shown in the middle panel of Fig. 5 (see Supporting Material).

Extension of the binding model to a physiological lipid composition

Annexin a5 generates a heat signal upon ligation of PS but not PC. Thus, to generate a reasonable signal, we scaled the PS content up to 40%. Because the lateral distributions of POPC and POPS are nearly random and relatively similar when they are bound by annexin (24), we could calculate

TABLE 1 Binding and thermodynamic parameters for annexin a5 titrations with 60:40 POPC/POPS and varying Ca^{2+}

	Ca^{2+} binding			Membrane binding[a]
	Without membrane	With membrane, high affinity	With membrane, low affinity	With saturating Ca^{2+} present
N	5.0 ± 0.4	2.0 ± 0.1	3.0 ± 0.1	$z = 46.5 \pm 0.1$
K (M^{-1})	3100 ± 300	410,000 ± 120,000	5800 ± 100	78,000 ± 4000
K_D (μM)	330 ± 40	2.4 ± 1.0	170 ± 10	13 ± 1
ΔH (kcal/mol)	−2.4 ± 0.2	3.8 ± 0.2	−13.4 ± 0.4	−17.3 ± 0.1
$T\Delta S$ (kcal/mol)	2.2 ± 0.2	11.2 ± 0.3	−8.5 ± 0.4	−10.9 ± 0.1
ΔG (kcal/mol)	−4.6 ± 0.1	−7.4 ± 0.2	−4.9 ± 0.1	−6.4 ± 0.1

The reported error represents 95% confidence intervals.
[a]The affinity for annexin to bind membrane in the absence of Ca^{2+} was calculated to be $K_L = (2.1 \pm 0.3) \times 10^1\ M^{-1}$ ($K_{D,L} = 50 \pm 20$ mM).

the affinities of annexin a5 for other ratios of POPS/POPC from the partition function (Eqs. 1 and 2). We then carried out ITC experiments with levels of PS such as those found at the inner leaflet of the plasma membrane (~20%), but by using the same partition function approach (to represent all the annexin a5 states), we could analyze the consequently smaller and noisier signal (Fig. 6, *left*). A reduction in the acidic lipid content would consequently reduce the binding affinity, but if the total lipid content were increased to maintain the same exposed PS concentrations, the same affinity of Ca^{2+}-saturated annexin a5 for POPC/POPS (80:20) would be predicted, and indeed, that is what we found (Fig. 6, *left*, and Table 2). The number of Ca^{2+} sites (n) varied with the lipid composition. Annexin a5 and Ca^{2+} were incubated together and POPC/POPS (80:20) was injected into this suspension to define the K_{app}. This titration had a consequently more muted curvature and heat response compared with the equivalent titration with 60:40 POPC/POPS because fewer PS molecules were distributed under each annexin a5 molecule due to the reduced amount of PS bound by each annexin (Fig. 6, *right*). The number of lipids bound by annexin (z) also varied with the lipid composition.

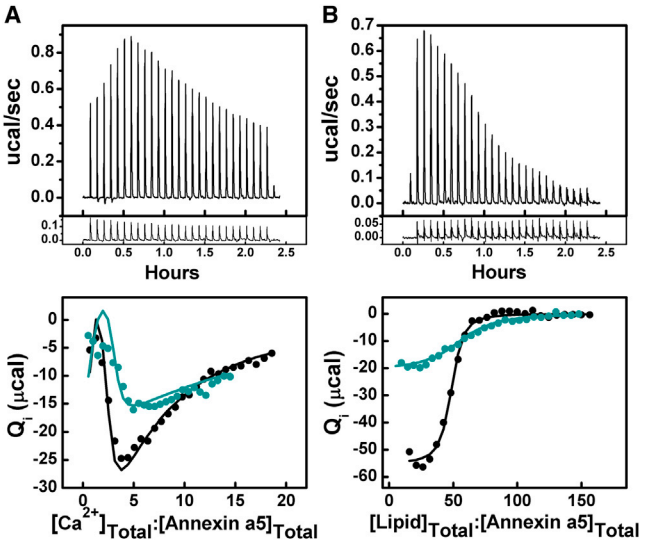

FIGURE 6 (*A*) Results of the titration of 24 μM annexin a5 with Ca^{2+} in the presence of 2 mM total lipid as LUVs made of a 60:40 mixture of POPC/POPS at 18°C (*solid black circles*). Results of the titration of 30 μM annexin a5 with Ca^{2+} in the presence of 4 mM total lipid as LUVs made of a 80:20 mixture of POPC/POPS at 18°C (*solid cyan circles*). Top: (*Upper Frame*) Raw ITC data from the titration of 30 μM annexin a5 with Ca^{2+} in the presence of 4 mM total lipid made of a mixture of 80:20 POPC/POPS at 18°C. (*Lower Frame*) Heat of dilution data (control). Bottom: Integrated heats of binding displayed as a function of ligand/protein ratio of annexin a5 with Ca^{2+} in the presence of 2 mM total lipid made of a mixture of 60:40 POPC/POPS (*solid black circles*) and in the presence of 4 mM total lipid made of a mixture of 80:20 POPC/POPS (*solid cyan circles*). (*B*) Results of the titration of 30 μM annexin a5 with lipid as LUVs made of a 60:40 mixture of POPC/POPS in the presence of 0.75 mM Ca^{2+} (*solid black circles*) at 15°C. Results of the titration of 20 μM annexin a5 with lipid as LUVs made of a 80:20 mixture of POPC/POPS in the presence of 2 mM Ca^{2+} (*solid cyan circles*) at 15°C. Top: (*Upper Frame*) Raw ITC data from the titration of 20 μM annexin a5 with lipid composed of a mixture of 80:20 POPC/POPS in the presence of 2 mM Ca^{2+} at 15°C. (*Lower Frame*) Heat of dilution data (control). Bottom: Integrated heats of binding displayed as a function of ligand/protein ratio of both annexin a5 with lipid composed of a 60:40 POPC/POPS mixture (*solid black circles*) and 80:20 POPC/POPS mixture (*solid cyan circles*) in the presence of 0.75 mM and 2 mM Ca^{2+}, respectively.

DISCUSSION

Ca^{2+} stimulates the membrane association of annexin (5,11,14,19–20,41–47). The model we propose is consistent with all of these observations, and suggests that there is a dynamic redistribution of protein conformational states upon Ca^{2+} influx (48–49). We have simplified this redistribution in our model to switching primarily between two conformational states: one free in solution and one membrane bound. We assume two states to represent two populations of conformers (48). This simplification allows us to describe the binding process in terms of a minimal number of binding constants.

The binding model we present is a type of allosteric transition, a theme common to biological function (48,50–54). A cooperative response in such a model is due to redistribution of the protein's conformational states, where the basal state (ligand-free conformation of the protein) that predominates is the solution state. There also exists a lower-probability but higher-affinity conformation for ligand (Ca^{2+}) that is the membrane-associated state. Both states have multiple binding sites for the ligand (Ca^{2+}). Similarly to most globular proteins, annexin a5 is in dynamic conformational equilibrium (49), and even in the absence of Ca^{2+}, some of the conformations will weakly associate with the membrane (25,35). The conformational change need not be a gross change in the structure of the protein—sometimes a subtle redistribution of conformers will suffice (28). It is important to note that our thermodynamic findings cannot (and do not) provide specific structural mechanistic details about the conformational change. Rather, they serve to illustrate the functional details of a possible mechanism, i.e., the annexin a5 binding response. Annexins have the ability to undergo dramatic conformational changes in the presence and absence of Ca^{2+} under both extreme and near-physiological conditions (12,55–57). The surprisingly low-heat-capacity change of some annexins measured in denaturation experiments (9) is also consistent with a structural malleability and potential for allosterism.

This annexin-binding response may be visualized traversing either side of the thermodynamic cycle (Fig. 1). The probability of annexin a5 binding Ca^{2+} in solution at physiological conditions is very low due to its K_D of 330 μM (see Table 1). During a Ca^{2+} influx, assuming a peak Ca^{2+} level of ~10–20 μM, <3–5% of annexin would be bound in solution. This binding step is weakly favorable from both an enthalpic and an entropic standpoint. The

TABLE 2 Binding and thermodynamic parameters for annexin a5 titrations with 80:20 POPC/POPS and varying Ca^{2+}

	Ca^{2+} binding		Membrane binding[a]
	With membrane, high affinity	With membrane, low affinity	With saturating Ca^{2+} present (2 mM)
N	3.0 ± 0.1	10.0 ± 0.7	$z = 56.6 \pm 0.4$
K (M^{-1})	500,000 ± 193,000	970 ± 70	13,500 ± 680
K_D (μM)	2.0 ± 1.0	1000 ± 80	74 ± 3
ΔH (kcal/mol)	1.5 ± 0.1	−7.3 ± 0.8	−13.30 ± 0.09
$T\Delta S$ (kcal/mol)	9.1 ± 0.2	−3.3 ± 0.8	−7.85 ± 0.09
ΔG (kcal/mol)	−7.6 ± 0.2	−4.0 ± 0.1	−5.44 ± 0.02

The reported error represents 95% confidence intervals.
[a]The affinity for annexin to bind membrane in the absence of Ca^{2+} was calculated to be $K_L = (1.6 \pm 0.3) \times 10^1\ M^{-1}$ ($K_{D,L} = 60 \pm 30$ mM).

entropic contribution may stem from the liberation of waters of hydration and associated ions of Ca^{2+} upon chelation. On this path of the thermodynamic cycle, annexin a5 binds Ca^{2+} and then membrane. The Ca^{2+}-bound annexin a5 is primed to interact with acidic membranes, as evidenced by the large, favorable enthalpic contribution to binding. When 80:20 POPC/POPS liposomes were titrated into saturating Ca^{2+}, the enthalpic contribution to binding was reduced because less PS is probable under each annexin in comparison with the analogous 60:40 POPC/POPS titration (Fig. 6; compare Table 1 and Table 2). Interestingly, the entropic contribution is very unfavorable for this step whether the ratio is 60:40 or 80:20, which is surprising considering that membrane ligation would be predicted to be highly entropically driven due to its associated waters and ions. This Ca^{2+}-primed annexin may lose its conformational pliability upon membrane binding (28), but gain membrane-binding specificity. It is the higher affinity of Ca^{2+}-bound annexin a5 for membrane compared with the relatively low affinity of annexin a5 for Ca^{2+} alone that then drives the protein to its fully bound state. We conclude that the membrane-bound conformer of the protein is sensitive to membrane composition based on a comparison of the Ca^{2+}-bound, membrane-binding step of annexin a5 for POPC/POPS (60:40) and POPC/POPS (80:20). The coupling of membrane composition to Ca^{2+} ligation is apparent by the greater number of Ca^{2+} sites induced by the presence of POPC/POPS (80:20) and hence the need for more Ca^{2+} to saturate the protein compared with POPC/POPS (60:40). Membrane composition thus altered both the number of lipids bound (z) and the number of Ca^{2+} sites (n), suggesting a membrane-based responsiveness of annexin a5 in the coupling of Ca^{2+} and membrane binding.

This coupling of Ca^{2+} binding to membrane composition also becomes apparent by traversing the other leg of the thermodynamic cycle where membrane and then Ca^{2+} are bound (Fig. 1). Upon the low-probability event of membrane ligation, the protein now differentiates its Ca^{2+}-binding response such that there are both high and low Ca^{2+} affinities within the protein compared with the undifferentiated solution-state affinities for Ca^{2+}. This differentiation is dependent on membrane composition, with two high-affinity and three low-affinity Ca^{2+}-sites in the presence of POPC/POPS (60:40), and three high-affinity and 10 low-affinity Ca^{2+}-sites in the presence of POPC/POPS (80:20). This membrane-bound-dependent differentiation in Ca^{2+} binding extends to its distinct thermodynamic profile, as the high-Ca^{2+}-affinity state is now entropically driven because it is endothermic with either membrane composition and increasingly endothermic with PS density (Fig. 6; Tables 1 and 2). Although there are numerous low-affinity Ca^{2+} sites that, similarly to solution-state binding, are exothermic, it is the higher-affinity, entropically driven, membrane-bound state that shifts the equilibrium to bind both Ca^{2+} and membrane. The total PS available during the 80:20 POPC/POPS titrations was conserved with that of the 60:40 POPC/POPS liposomes by increasing the total lipid concentration. The resultant measured free energies of Ca^{2+} binding in the presence of membrane were thus approximately the same for either lipid composition. Between these experiments, the total PS content was conserved but the binding stoichiometry differed. Thus, we conclude that it is the distribution of acidic lipids, and not the acidic lipid content, to which annexin responds with differential membrane sensitivity to Ca^{2+}. Each injection point and resultant heat in ITC is a representation of the dynamic equilibrium in which both sides of the thermodynamic cycle are represented when both Ca^{2+} and membrane are present. Therefore, both sides of the thermodynamic cycle are represented in the binding profile and in the partition function used to analyze the data and deconvolute the probability of either path.

To illustrate this interdependence of binding that arises from weak membrane association and results in cooperative calcium ligation, we plotted the fraction of each ligated protein state (free, bound to Ca^{2+} in solution, bound to Ca^{2+} and membrane, or bound only to membrane) in Fig. 7. The experimentally derived association constants used were for a membrane consisting of POPC/POPS (60:40) LUVs (Table 1). The total membrane concentration was fixed to create three different scenarios: low concentration, high concentration, and experimental concentration (Fig. 7, *top*, *middle*, and *bottom* panels, respectively). Within each distribution plot of the above membrane concentrations, the fraction of each protein species was plotted

as a function of Ca^{2+}. Upon an increase in the Ca^{2+} concentration, the protein redistributed between solution and membrane-associated states to varying degrees. If the initial membrane association in the absence of Ca^{2+} was too weak, such as when the membrane concentration was low (e.g., 0.02 mM total lipid, as in Fig. 7, *top panel*), the protein remained predominantly in the solution state even at high concentrations of Ca^{2+} (i.e., calcium and membrane did not link up). If the lipid concentration was high (e.g., 200 mM total lipid, as in Fig. 7, *middle panel*), the protein was initially bound predominantly to membrane and remained that way (though also bound to Ca^{2+}). The binding of Ca^{2+} in either case was not cooperative.

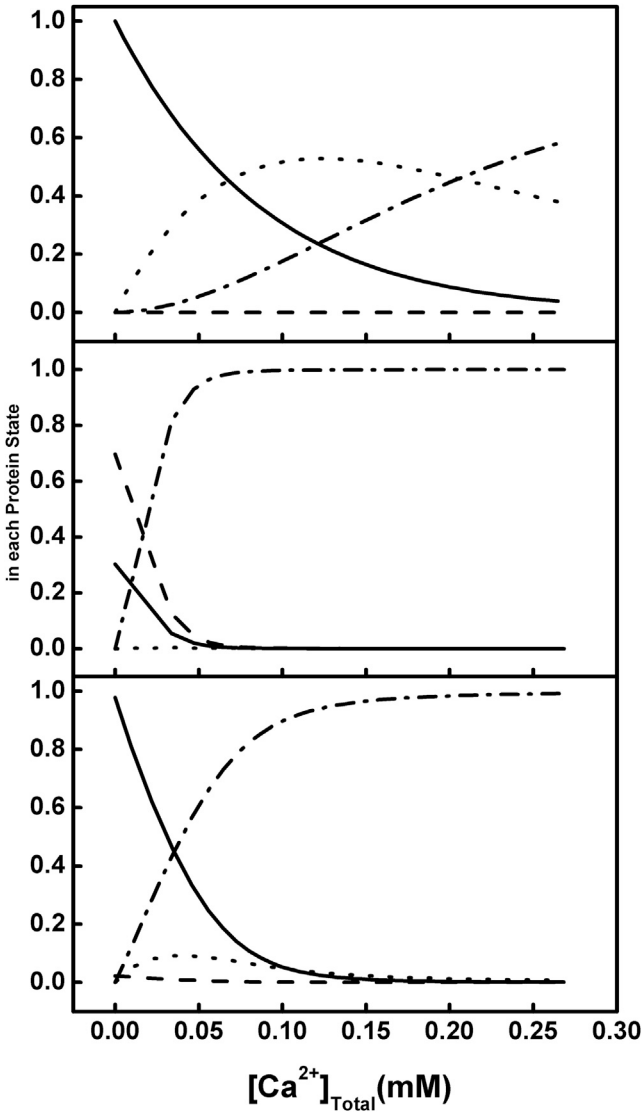

FIGURE 7 Distribution of all possible states of annexin a5 as a function of increasing concentrations of Ca^{2+}. Solid line: ligand-free protein; dotted line: Ca^{2+}-bound protein; dashed line: lipid-bound protein; dot-dashed line: Ca^{2+} and lipid-bound protein. (*Top*) Distributions calculated using the binding constants in Table 1 for 24 μM annexin a5 assuming a total lipid concentration of 0.02 mM. (*Middle*) Distributions similarly calculated for 24 μM annexin a5 assuming a total lipid concentration of 200 mM. (*Bottom*) Distributions similarly calculated for 24 μM annexin a5 in the presence of 2 mM total lipid.

The total membrane concentration at which our experimental results (Fig. 4) were obtained resides between these two scenarios of low and high membrane concentrations (2 mM total lipid or 400 μM exposed PS, as in Fig. 7, *bottom panel*). This creates an exquisitely sensitive response, as evidenced by the redistribution of the protein over a very small concentration range of Ca^{2+} from being only Ca^{2+}-bound in solution to being both Ca^{2+}-bound and membrane-bound (see Fig. 4, *bottom panel*, for membrane- and Ca^{2+}-bound states). Note that the fraction of protein associated with the membrane in the absence of Ca^{2+} is not very significant (~2%; see Fig. 7, *bottom panel*, *dashed line* y-intercept), yet the switch between being bound to Ca^{2+} in solution or bound to both membrane and Ca^{2+} is strongly modulated by this slight Ca^{2+}-free membrane association. We suggest that this switch is physiologically relevant because it provides a sensitive means of communicating binding information.

To further illustrate the sensitivity of how weak membrane association conveys cooperativity, the binding isotherms of Figs. 3 and 4 (*bottom panels*) are overlapped in Fig. 8. The impact of membrane association becomes apparent as membrane-associated annexin a5 is saturated with Ca^{2+} at lower Ca^{2+} concentrations compared with the solution state. The Ca^{2+} saturation exhibits the classic lag and rise of a cooperative binding process. At a small Ca^{2+} concentration of 100 μM, the fractional saturation of the protein changes from only 20% for solution-state protein to 40% when in the presence of membrane. This is very similar to our previous finding with annexin a5 utilizing the Ca^{2+} mimic Tb^{3+} (28). The primary differences between this work and the previous work are the protein-cation affinity (K_0) resulting from the fits, the differentiation of the membrane-associated affinities for cation (K_1 to K_{1a} and

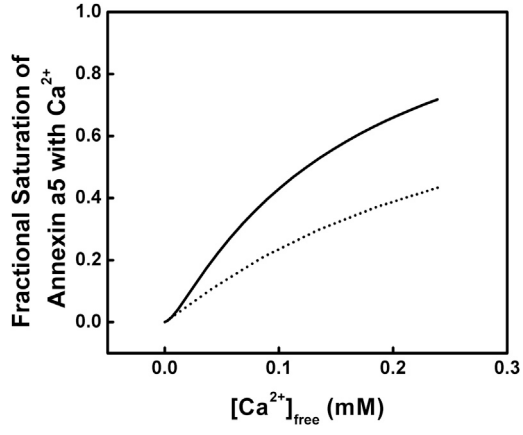

FIGURE 8 Overlay of the binding isotherms for Ca^{2+} binding to annexin a5 in the solution state (*dotted line*) and membrane-bound state (*solid line*, [L] = 2 mM).

K_{1b}), and the protein/lipid ratios. The first difference may be due to the greater charge density of Tb^{3+} compared with Ca^{2+}, which is the result of having a similar ionic radius but higher charge. The second difference reflects differences in the sign of the heats of interaction upon Ca^{2+} ligation revealed here by ITC. The third is due to an underestimation of the protein/lipid ratio (20 lipids/protein), which led to an overestimation of the K_L in the previous work, as an underestimation of the protein/lipid ratio leads to a resultant greater concentration of free lipid remaining after protein is bound. In this study, using ITC to directly define the z term of protein/lipid stoichiometry enabled us to define the K_L term more accurately.

CONCLUSIONS

For annexin a5, whether in the solution state or the membrane-bound state, binding of Ca^{2+} is independent (the binding of one Ca^{2+} does not impact the binding of another Ca^{2+}). However, the conformers of membrane-associated annexin have a greater affinity for Ca^{2+} compared with the solution-state conformers of the protein. Because the membrane-bound state of the protein has a greater affinity for Ca^{2+} than does the solution-state protein, upon Ca^{2+} influx, the membrane bound state binds Ca^{2+} with greater probability. Thus, the membrane-associated (but Ca^{2+}-free) population of protein is depleted upon addition of Ca^{2+}. This state then becomes repopulated by a shift in equilibrium, giving the appearance of an initial lag in Ca^{2+} binding (due to shifting and replenishing; Fig. 8). If the protein is mostly or completely membrane bound, an independent (hyperbolic-shaped) Ca^{2+} binding response will result, and binding will occur with the higher affinity of this membrane-associated state. However, if a relatively small population of the protein is membrane-associated (in the initial absence of Ca^{2+}), a cooperative Ca^{2+} binding profile will result. Upon Ca^{2+} influx, the protein will transition from an unbound to bound state over a much smaller concentration range of Ca^{2+} than is found in an independent Ca^{2+}-binding site scenario. This cooperative response is possible only if the membrane-bound state of the protein is populated to a relatively low extent in the absence of Ca^{2+}. Thus, weak membrane association in the absence of Ca^{2+} is one means of achieving a cooperative (switch-like) binding response for the peripheral membrane protein annexin a5.

SUPPORTING MATERIAL

Supporting analysis and four figures are available at http://www.biophysj.org/biophysj/supplemental/S0006-3495(13)00446-3.

We thank Paulo Almeida for discussions.

This work was supported in part by the National Institutes of Health (grant GM64443 to A.H.). A.H. received support from a National Science Foundation CAREER Award (MCB-0845676).

REFERENCES

1. Hinderliter, A., P. F. F. Almeida, …, R. L. Biltonen. 2001. Domain formation in a fluid mixed lipid bilayer modulated through binding of the C2 protein motif. *Biochemistry.* 40:4181–4191.
2. Hinderliter, A., R. L. Biltonen, and P. F. F. Almeida. 2004. Lipid modulation of protein-induced membrane domains as a mechanism for controlling signal transduction. *Biochemistry.* 43:7102–7110.
3. Almeida, P. F. F., A. Pokorny, and A. Hinderliter. 2005. Thermodynamics of membrane domains. *Biochim. Biophys. Acta.* 1720:1–13.
4. Murphy, J., K. Knutson, and A. Hinderliter. 2009. Protein-lipid interactions role of membrane plasticity and lipid specificity on peripheral protein interactions. *Methods Enzymol.* 466:431–453.
5. Raynal, P., and H. B. Pollard. 1994. Annexins: the problem of assessing the biological role for a gene family of multifunctional calcium- and phospholipid-binding proteins. *Biochim. Biophys. Acta.* 1197:63–93.
6. Moss, S. E., and R. O. Morgan. 2004. The annexins. *Genome Biol.* 5:219.
7. Zschörnig, O., F. Opitz, and M. Müller. 2007. Annexin A4 binding to anionic phospholipid vesicles modulated by pH and calcium. *Eur. Biophys. J.* 36:415–424.
8. Tait, J. F., D. F. Gibson, and C. Smith. 2004. Measurement of the affinity and cooperativity of annexin V-membrane binding under conditions of low membrane occupancy. *Anal. Biochem.* 329:112–119.
9. Rosengarth, A., J. Rösgen, …, V. Gerke. 1999. A comparison of the energetics of annexin I and annexin V. *J. Mol. Biol.* 288:1013–1025.
10. Rosengarth, A., J. Rösgen, …, V. Gerke. 2001. Folding energetics of ligand binding proteins II. Cooperative binding of Ca^{2+} to annexin I. *J. Mol. Biol.* 306:825–835.
11. Gilmanshin, R., C. E. Creutz, and L. K. Tamm. 1994. Annexin IV reduces the rate of lateral lipid diffusion and changes the fluid phase structure of the lipid bilayer when it binds to negatively charged membranes in the presence of calcium. *Biochemistry.* 33:8225–8232.
12. Isas, J. M., J.-P. Cartailler, …, H. T. Haigler. 2000. Annexins V and XII insert into bilayers at mildly acidic pH and form ion channels. *Biochemistry.* 39:3015–3022.
13. Isas, J. M., R. Langen, …, W. L. Hubbell. 2002. Structure and dynamics of a helical hairpin and loop region in annexin 12: a site-directed spin labeling study. *Biochemistry.* 41:1464–1473.
14. Isas, J. M., R. Langen, …, H. T. Haigler. 2004. Structure and dynamics of a helical hairpin that mediates calcium-dependent membrane binding of annexin B12. *J. Biol. Chem.* 279:32492–32498.
15. Jeppesen, B., C. Smith, …, J. F. Tait. 2008. Entropic and enthalpic contributions to annexin V-membrane binding: a comprehensive quantitative model. *J. Biol. Chem.* 283:6126–6135.
16. Junker, M., and C. E. Creutz. 1993. Endonexin (annexin IV)-mediated lateral segregation of phosphatidylglycerol in phosphatidylglycerol/phosphatidylcholine membranes. *Biochemistry.* 32:9968–9974.
17. Junker, M., and C. E. Creutz. 1994. $Ca^{(2+)}$-dependent binding of endonexin (annexin IV) to membranes: analysis of the effects of membrane lipid composition and development of a predictive model for the binding interaction. *Biochemistry.* 33:8930–8940.
18. Langen, R., J. M. Isas, …, W. L. Hubbell. 1998. Membrane-mediated assembly of annexins studied by site-directed spin labeling. *J. Biol. Chem.* 273:22453–22457.
19. Mailliard, W. S., H. Luecke, and H. T. Haigler. 1997. Annexin XII forms calcium-dependent multimers in solution and on phospholipid bilayers: a chemical cross-linking study. *Biochemistry.* 36:9045–9050.
20. Patel, D. R., C. C. Jao, …, H. T. Haigler. 2001. Calcium-dependent binding of annexin 12 to phospholipid bilayers: stoichiometry and implications. *Biochemistry.* 40:7054–7060.
21. Patel, D. R., J. M. Isas, …, H. T. Haigler. 2005. The conserved core domains of annexins A1, A2, A5, and B12 can be divided into two groups with different Ca^{2+}-dependent membrane-binding properties. *Biochemistry.* 44:2833–2844.

22. Zaks, W. J., and C. E. Creutz. 1991. Ca(2+)-dependent annexin self-association on membrane surfaces. *Biochemistry.* 30:9607–9615.

23. Morgan, R. O., and M.-P. Fernández. 1995. Molecular phylogeny of annexins and identification of a primitive homologue in *Giardia lamblia*. *Mol. Biol. Evol.* 12:967–979.

24. Almeida, P. F., A. Best, and A. Hinderliter. 2011. Monte Carlo simulation of protein-induced lipid demixing in a membrane with interactions derived from experiment. *Biophys. J.* 101:1930–1937.

25. Vats, K., K. Knutson, …, E. D. Sheets. 2010. Peripheral protein organization and its influence on lipid diffusion in biomimetic membranes. *ACS Chem. Biol.* 5:393–403.

26. Bouter, A., C. Gounou, …, A. R. Brisson. 2011. Annexin-A5 assembled into two-dimensional arrays promotes cell membrane repair. *Nat Commun.* 2:270.

27. Buzhynskyy, N., M. Golczak, …, A. R. Brisson. 2009. Annexin-A6 presents two modes of association with phospholipid membranes. A combined QCM-D, AFM and cryo-TEM study. *J. Struct. Biol.* 168:107–116.

28. Almeida, P. F. F., H. Sohma, …, A. Hinderliter. 2005. Allosterism in membrane binding: a common motif of the annexins? *Biochemistry.* 44:10905–10913.

29. Plager, D. A., and G. L. Nelsestuen. 1994. Direct enthalpy measurements of the calcium-dependent interaction of annexins V and VI with phospholipid vesicles. *Biochemistry.* 33:13239–13249.

30. Fezoua-Boubegtiten, Z., B. Desbat, …, S. Lecomte. 2011. Effect of Mg2+ versus Ca2+ on the behavior of annexin A5 in a membrane-bound state. *Eur. Biophys. J.* 40:641–649.

31. Freire, E., A. Schön, and A. Velazquez-Campoy. 2009. Isothermal titration calorimetry: general formalism using binding polynomials. *Methods Enzymol.* 455:127–155.

32. Hayes, M. J., and S. E. Moss. 2004. Annexins and disease. *Biochem. Biophys. Res. Commun.* 322:1166–1170.

33. Gerke, V., and S. E. Moss. 1997. Annexins and membrane dynamics. *Biochim. Biophys. Acta.* 1357:129–154 (BBA).

34. Gerke, V., and S. E. Moss. 2002. Annexins: from structure to function. *Physiol. Rev.* 82:331–371.

35. Torrecillas, A., J. Laynez, …, J. C. Gómez-Fernández. 2004. Calorimetric study of the interaction of the C2 domains of classical protein kinase C isoenzymes with Ca2+ and phospholipids. *Biochemistry.* 43:11727–11739.

36. Shahin, V., D. Datta, …, J. M. Edwardson. 2008. Synaptotagmin perturbs the structure of phospholipid bilayers. *Biochemistry.* 47:2143–2152.

37. Takahashi, H., V. Shahin, …, J. M. Edwardson. 2010. Interaction of synaptotagmin with lipid bilayers, analyzed by single-molecule force spectroscopy. *Biophys. J.* 99:2550–2558.

38. Wyman, J., and S. J. Gill. 1990. Binding and Linkage: Functional Chemistry of Biological Molecules. University Science Books, Mill Valley, CA.

39. Wiseman, T., S. Williston, …, L. N. Lin. 1989. Rapid measurement of binding constants and heats of binding using a new titration calorimeter. *Anal. Biochem.* 179:131–137.

40. Campos, B., Y. D. Mo, …, B. A. Seaton. 1998. Mutational and crystallographic analyses of interfacial residues in annexin V suggest direct interactions with phospholipid membrane components. *Biochemistry.* 37:8004–8010.

41. Chasserot-Golaz, S., N. Vitale, …, M. F. Bader. 2005. Annexin 2 promotes the formation of lipid microdomains required for calcium-regulated exocytosis of dense-core vesicles. *Mol. Biol. Cell.* 16:1108–1119.

42. Janshoff, A., M. Ross, …, C. Steinem. 2001. Visualization of annexin I binding to calcium-induced phosphatidylserine domains. *ChemBioChem.* 2:587–590.

43. Lu, Y., M. D. Bazzi, and G. L. Nelsestuen. 1995. Kinetics of annexin VI, calcium, and phospholipid association and dissociation. *Biochemistry.* 34:10777–10785.

44. Meers, P., and T. Mealy. 1993. Calcium-dependent annexin V binding to phospholipids: stoichiometry, specificity, and the role of negative charge. *Biochemistry.* 32:11711–11721.

45. Meers, P., and T. Mealy. 1993. Relationship between annexin V tryptophan exposure, calcium, and phospholipid binding. *Biochemistry.* 32:5411–5418.

46. Megli, F. M., M. Selvaggi, …, R. Huber. 1998. The calcium-dependent binding of annexin V to phospholipid vesicles influences the bilayer inner fluidity gradient. *Biochemistry.* 37:10540–10546.

47. Babiychuk, E. B., and A. Draeger. 2000. Annexins in cell membrane dynamics. Ca(2+)-regulated association of lipid microdomains. *J. Cell Biol.* 150:1113–1124.

48. Monod, J., J. Wyman, and J.-P. Changeux. 1965. On the nature of allosteric transitions: a plausible model. *J. Mol. Biol.* 12:88–118.

49. Tobi, D., and I. Bahar. 2005. Structural changes involved in protein binding correlate with intrinsic motions of proteins in the unbound state. *Proc. Natl. Acad. Sci. USA.* 102:18908–18913.

50. Kenakin, T. 2004. G-protein coupled receptors as allosteric machines. *Receptors Channels.* 10:51–60.

51. Kenakin, T. 2007. Allosteric theory: taking therapeutic advantage of the malleable nature of GPCRs. *Curr. Neuropharmacol.* 5:149–156.

52. Kenakin, T. 2011. Functional selectivity and biased receptor signaling. *J. Pharmacol. Exp. Ther.* 336:296–302.

53. Vaidehi, N., and T. Kenakin. 2010. The role of conformational ensembles of seven transmembrane receptors in functional selectivity. *Curr. Opin. Pharmacol.* 10:775–781.

54. Garcia, H. G., J. Kondev, …, R. Phillips. 2011. Thermodynamics of biological processes. *Methods Enzymol.* 492:27–59.

55. Kim, Y. E., J. M. Isas, …, R. Langen. 2005. A helical hairpin region of soluble annexin B12 refolds and forms a continuous transmembrane helix at mildly acidic pH. *J. Biol. Chem.* 280:32398–32404.

56. Köhler, G., U. Hering, …, K. Arnold. 1997. Annexin V interaction with phosphatidylserine-containing vesicles at low and neutral pH. *Biochemistry.* 36:8189–8194.

57. Silvestro, L., and P. H. Axelsen. 1999. Fourier transform infrared linked analysis of conformational changes in annexin V upon membrane binding. *Biochemistry.* 38:113–121.